Chemistry & Biology 13, 711–722, July 2006 DOI 10.1016/j.chembiol.2006.05.008

MASPIT: Three-Hybrid Trap for Quantitative Proteome Fingerprinting of Small Molecule-Protein Interactions in Mammalian Cells

Maureen Caligiuri,[1] Lisa Molz,[1] Qing Liu,[1] Faith Kaplan,[1] Jimmy P. Xu,[1] Jiangwen Z. Majeti,[1] Rebeca Ramos-Kelsey,[1] Krishna Murthi,[1] Sam Lievens,[2] Jan Tavernier,[2] and Nikolai Kley[1,3,*]

[1] GPC Biotech Incorporated
610 Lincoln Street
Waltham, Massachusetts 02451

[2] Flanders Interuniversity Institute for Biotechnology
VIB09
Department of Medical Protein Research
Faculty of Medicine and Health Sciences
Ghent University
A. Baertsoenkaai 3
B-9000 Ghent
Belgium

Summary

Organic small molecules generally act by perturbing the function of one or more cellular target proteins, the identification of which is essential to an understanding of the molecular basis of drug action. Here we describe the application of methotrexate-linked small molecule ligands to a mammalian three-hybrid interaction trap for proteome-wide identification of small molecule targets, quantification of the targeting potency of unmodified small molecules for such targets in intact cells, and screening for inhibitors of small molecule-protein interactions. During the course of this study we also identified the pyrido[2,3-d]pyrimidine PD173955, a known SRC kinase inhibitor, as a potent inhibitor of several ephrin receptor tyrosine kinases. This finding could perhaps be exploited in the design of inhibitors for this kinase subfamily, members of which have been implicated in the pathogenesis of various diseases, including cancer.

Introduction

Mechanism of action studies play an important role in understanding the biological activity profiles of small molecules, in evaluating their potential as chemical genetics tools to study protein functions, and in the discovery and/or characterization of drug candidates and their therapeutic potential. Recent chemical proteomics studies have revealed that small molecules, including marketed drugs and drug candidates, are often less selective than previously recognized [1–6]. Even structurally highly related molecules may have significantly distinct target profiles, underscoring the general difficulty in predicting the composite target profile of a small molecule and, consequently, the importance of proteome-wide approaches in elucidating the mechanism of action of organic small molecules.

*Correspondence: nikolai.kley@gpc-biotech.com
[3] Lab address: http://www.gpc-biotech.com

Various chemical proteomic methods for the identification of small molecule-protein interactions have been described in recent years. These include affinity chromatography-based methods, activity-based proteome profiling (ABPP), phage display, protein arrays, and yeast three-hybrid (Y3H) [1–4, 7–10]. Y3H is an extension of yeast two-hybrid (Y2H), which was developed by Fields and Song [11]. In Y2H, the interaction of two proteins is detected by linking their association to the transcriptional activation of a reporter gene. In Y3H, protein complex formation is mediated by a small molecule hybrid ligand [3, 12, 13]. Methotrexate (MTX) hybrid ligands have been shown to successfully display small molecules in Y3H, thereby enabling the identification of candidate cellular targets that these molecules bind to [13–15]. An attractive feature of Y3H is that it can be automated at various steps and used to perform large-scale screens of proteome cDNA libraries, specific protein classes, or mutants of the same protein [3]. Target fingerprints identified in this manner can lead to new insights into structure-activity relationships (SARs) of small molecules. In addition, they can identify a drug-resistant variant(s) of a target protein, which could be used to explore its role in mediating a pharmacological effect of interest, or mutations in a target protein that might emerge in drug-resistant variants during therapy [16, 17]. As with all technologies, however, Y3H is subject to certain limitations [3]. For instance, it is limited to the detection of interactions with proteins or protein domains that effectively translocate into the nucleus. One drawback of using yeast cells as a host for a three-hybrid system is that these cells are generally not very permeable to nonhybrid small molecules. This prevents the use of Y3H in determining the ability of compounds to interfere with or actively reverse a specific hybrid ligand-target protein interaction and, hence, its use in ranking compounds with respect to their targeting potencies, as well as random screening for small molecule-protein interaction modifiers. Competitive screening assays would most ideally be performed in mammalian cells.

Here we describe the development of a mammalian three-hybrid system (M3H) that complements Y3H while circumventing some of its limitations. In an analogous strategy to that used in the Y3H system, we adapted a two-hybrid protein-protein interaction trap, MAPPIT [18, 19] (mammalian protein-protein interaction trap), to be used with methotrexate-based chemical dimerizers. MAPPIT is a complementation system in which the interaction of two fusion proteins ("bait" and "prey" proteins) restores ligand-dependent activation of JAK/STAT signaling to a signaling-deficient cytokine receptor (see Figure 1). Various types of protein-protein interactions have been detected with MAPPIT and reverse-MAPPIT [18, 20–23]. An important application of MAPPIT is in the de novo identification of protein-protein interactions using cDNA library screening, and this suggests that it might also prove applicable to the design of an M3H system for use in target identification. Another attractive feature of MAPPIT is that protein

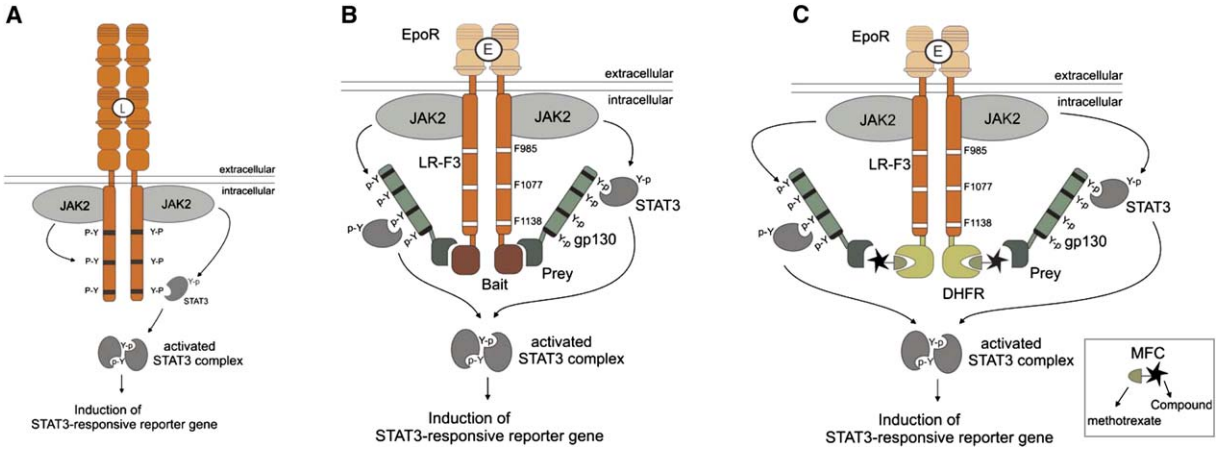

Figure 1. The MASPIT System

(A) The JAK-STAT signal transduction system. Phosphorylation of the cytokine receptor by activated JAK provides a STAT docking site. Recruited STAT is subsequently phosphorylated by JAK, leading to its activation.

(B) The MAPPIT system. Here the cytokine receptor is a chimera, including the ligand binding domain of the Epo receptor (EpoR) and the cytoplasmic domain of a mutated leptin receptor (LRF3), which lacks functional STAT3 recruitment sites. Complementation and restoration of JAK2/STAT3 signaling is achieved by interaction of a bait protein fused to the receptor and a prey protein fused to the C-terminal portion of gp130, which contains four STAT3 binding sites.

(C) The MASPIT system. eDHFR is fused to the chimeric receptor, enabling the display of an MTX hybrid ligand in which a small molecule is linked to MTX via a polyethylene glycol repeat (n = 5) linker/spacer. Interaction of this small molecule with a prey-gp130 protein leads to recruitment of a docking site for STAT3, which now can be phosphorylated by JAK2. Activation of JAK2 is triggered by binding of Epo to the extracellular domain of the chimeric receptor. Collectively, a productive small molecule-protein interaction in MASPIT restores an Epo-dependent activation of JAK2/STAT3 signaling and induction of the expression of a STAT3-responsive reporter gene.

interactions occur in the cytoplasm; therefore, no nuclear translocation of fusion proteins or small molecules would be required in a 3H version of it. Furthermore, interaction-triggered signal transmission is highly ligand regulated, which we reasoned could be of significant benefit in developing a robust M3H proteome cDNA library screening method with acceptable signal/noise ratios. Here we describe such a mammalian small molecule protein interaction trap (MASPIT) and its successful application to small molecule target identification and activity profiling of organic small molecules in intact cells.

Results

The MASPIT System

Figure 1 describes features of cytokine receptor-associated JAK/STAT signaling, the basic components of the MAPPIT system, as described previously [18], and the MASPIT system as developed in this study. As in the Y3H system we described earlier [3, 13], the MASPIT system used here employs an *Escherichia coli* DHFR (eDHFR) fusion protein for the display of a methotrexate fusion compound (MFC) in which a small molecule is connected to MTX via a polyethylene glycol (PEG) repeat linker/spacer. As outlined in Figure 1, a small molecule-protein interaction is detected as an erythropoietin (Epo)/MFC-dependent activation of JAK/STAT3 signaling, which can be monitored by measuring the activity of a reporter gene (e.g., luciferase) that is under the control of a STAT3-responsive rat pancreatitis-associated protein 1 (rPAP1) promoter. HEK293 or HEK293T (the latter express SV40 large T antigen) were used as host cells.

Use of MTX Hybrid Ligands Derived from Diverse Small Molecule Chemotypes

Figure 2 summarizes MASPIT interaction results for various types of small molecules and their known target proteins when these were transiently expressed in HEK293T cells. These compounds are as follows:

1. AP1867, which is an FK506 analog that specifically binds with high affinity a mutated form of FKBP12 ($FKBP12^{F36V}$) [24].
2. PD173955, which is a potent ABL kinase inhibitor [25, 26].
3. RGB-285961 and RGB-286147, which are potent inhibitors of CDK2. These compounds belong to a class of 1,3,6-trisubstituted-pyrazolopyrimidones [27]. We have recently shown that MFC derivatives of these compounds interact with CDK2 in Y3H [15].
4. RGB-285978, which is a potent inhibitor of cyclin-dependent kinases (CDKs) and GSK3. RGB-285978 belongs to the chemical class of indenopyrazoles [28, 29]. We have previously shown that a related member of this class (IP1) interacts with CDKs and GSK3 in Y3H [13].
5. E7070, which is an inhibitor of carbonic anhydrase (CAII) [30].

These small molecules were each coupled to MTX. The chemical structures of their MFC derivatives are shown in Figure 2A. MTX coupled to a small molecule was observed to retain high affinity for purified eDHFR, indicating that the PEG linker was attached to a suitable position on MTX (K_D in the picomolar to nanomolar range, as determined in BIACORE assays; data not shown). Given that MTX exhibits variable antiproliferative effects

A

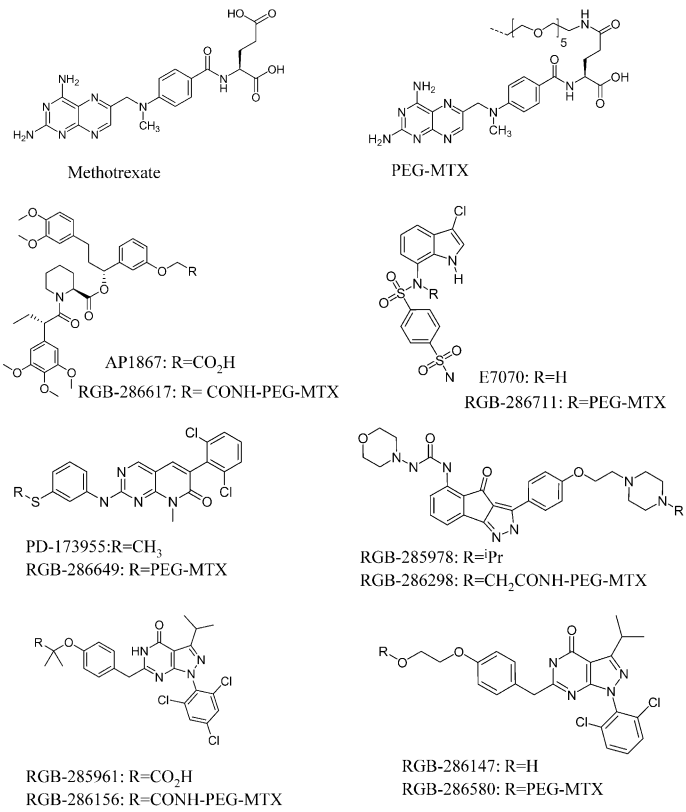

B

Methorexate Fusion Compound (MFC)	Target Protein	Luciferase reporter expression (fold induction)	HEK-293T IC50 (μM)
RGB-286617	FKBP12 ^{F36V}	305	>3
RGB-286649	ABL	359	>3
RGB-286156	CDK2	25	>3
RGB-286580	CDK2	20	>3
RGB-286298	GSK3β	7	>3
RGB-286711	CAII	49	>3

Figure 2. Detection of Small Molecule-Protein Interactions with MASPIT

(A) Small molecules and MFC derivatives used in this study.

(B) Effects of MFCs on HEK293T cell proliferation/viability (IC_{50}s were determined following 24 hr exposure to the MFC with the SRB assay or the Cell TiterGlo ATP luminescence assay) and induction of a STAT3-responsive luciferase reporter. For MASPIT studies, HEK293T cells were transiently transfected with the EpoR-LepRF3-DHFR bait, the rPAP-luciferase reporter, and the indicated gp130-target fusion vectors. The transfected cells were exposed to Epo in the presence or absence of the MFC. The MFC-dependent induction of the luciferase reporter is shown. The concentrations of MFCs used in this study were RGB-286649 at 0.01 μM, RGB-286617 and RGB-286711 at 0.1 μM, RGB-286156 at 0.2 μM, RGB-286580 at 0.3 μM, and RGB-286298 at 1 μM.

in mammalian cells (GI_{50}s range across the National Cancer Institute tumor cell panel, 0.3 to >30 μM; see http://www.dtp.nci.nih.gov/), we evaluated the effects of MTX and MFCs on HEK293T cell growth and viability. Neither MTX nor any of the MFCs exhibited antiproliferative or cytotoxic activities that would seemingly prevent their use in MASPIT (IC_{50}s > 3 μM at 24 hr incubation; see Figure 2B). Indeed, as summarized in Figure 2B, by 24 hr incubation, all MFCs induced a strong Epo-dependent expression of a STAT3-responsive luciferase reporter gene in HEK293T cells expressing the appropriate target protein (even at MFC concentrations well below their cell proliferation IC_{50}s; see also Figure 3).

As shown in Figure 3, MFC-induced reporter expression was dependent on (1) ligand/Epo activation of the chimeric EpoR-LepRF3-DHFR receptor, (2) MFC concentration, and (3) level of expression of the small-molecule target-gp130 fusion protein. For instance, in cells expressing FKBP12^{F36V}, the AP1867-MFC (RGB-286617) caused a dose-dependent induction of luciferase expression, which is dependent on the presence of Epo (Figure 3A). Similarly, MFCs for the ABL kinase inhibitor PD173955 (RGB-286649) and the CDK2 inhibitor RGB-285961 (RGB-286156) induced luciferase expression in a dose-dependent fashion (Figures 3B and 3C, respectively). As with RGB-286156 (Figure 3C), reporter activation was also time dependent (high levels of induction were observed for all MFCs within 24 hr; Figure 2B) and proportional to the level of expression of the gp130-prey fusion protein (CDK2 in this example). Similar results were obtained for other small molecule chemotypes, as illustrated by the dose-dependent induction of luciferase expression with RGB-286711 (Figure 3D), the MFC for the CAII inhibitor E7070. Collectively, the results described in Figures 2 and 3 indicate that MASPIT exhibits a broad dynamic range and that it accommodates small molecules that exhibit very different biological activities (targets and binding modes).

Proteome Screening and De Novo Identification of Small Molecule Protein Targets

Having established that MASPIT can be used to detect pairwise interactions of small molecules with their target proteins, we explored next its application to proteome scanning. For this purpose, we used genetically engineered HEK293 cells that stably express the EpoR-LepRF3-DHFR fusion protein and carry an integrated STAT3-responsive rPAP1-IL5 receptor (IL5R) reporter

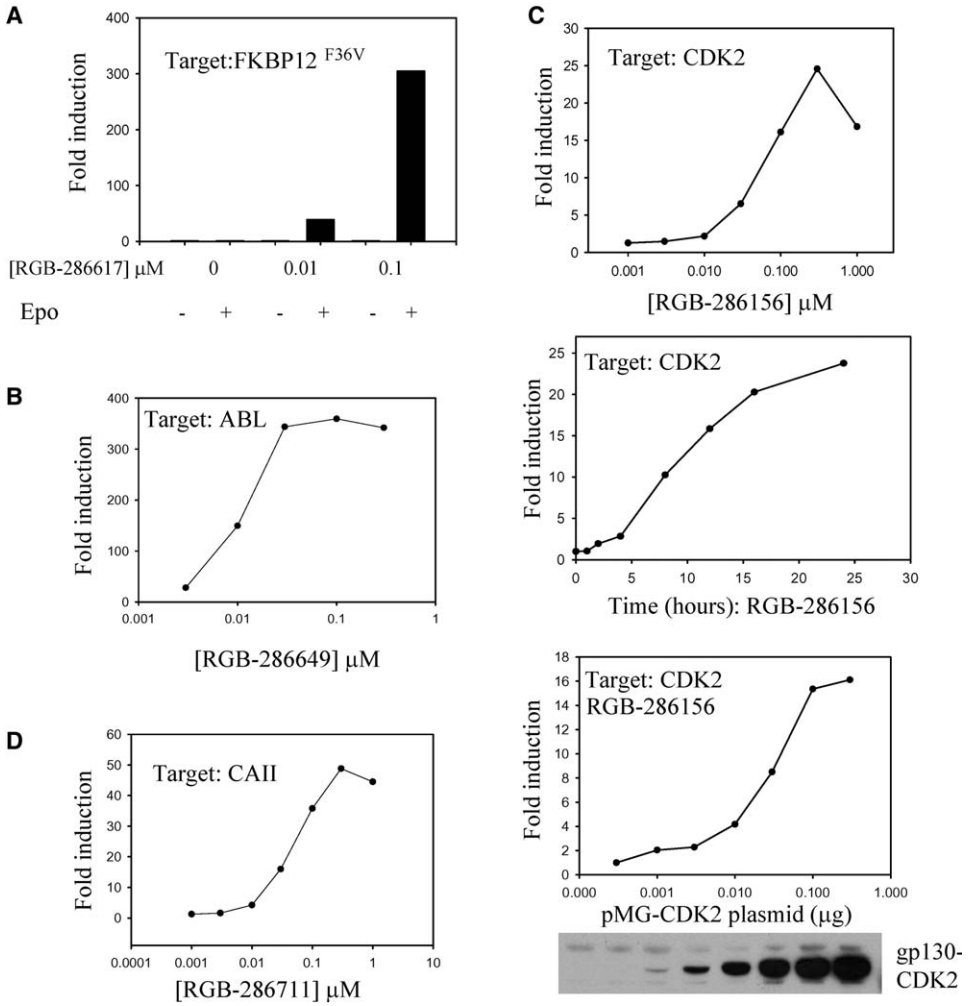

Figure 3. Component Dependence of the MASPIT System

(A) Dependence of MASPIT signaling on Epo and MFC. HEK293T cells were transiently transfected with vectors encoding the EpoR-LepRF3-DHFR bait, the rPAP1-luciferase reporter, and gp130-FKBP12^{F36V}, and a vector encoding β-galactosidase (for transfection efficiency normalization). Transfected cells were exposed to MFC at concentrations of 0.01 and 0.1 μM in the presence or absence of Epo for 24 hr. Normalized, MFC-dependent induction of the luciferase activity is shown.

(B–D) Dependence of MASPIT signaling on MFC concentration (B–D; 24 hr MFC exposure), time of MFC exposure (C, middle panel; RGB-286156 at 0.3 μM), and gp130-target expression levels (C, lower panel; RGB-286156 at 0.3 μM, 24 hr). HEK293T cells were transiently transfected as described above, but including the indicated gp130-target fusion vectors. The transfected cells were exposed to Epo in the presence or absence of the MFC, and MFC-dependent induction of the luciferase expression was determined.

gene [22]. The IL5R reporter used here lacked the cytoplasmic domain of the receptor; this avoids competition for JAK binding and removes potential receptor internalization motifs. Expression of this IL5R was monitored by flow cytometry using an anti-IL5R-specific monoclonal antibody. These recombinant HEK293 cells were also engineered to express a murine ecotropic virus receptor for viral infection applications. A representative experiment in which the integrated rPAP1-IL5R reporter is activated in response to interaction of ABL with the MFC of the ABL inhibitor PD173955 [25, 26, 31], RGB-286649, is shown in Figure 4A. Treatment of ABL-gp130-expressing cells with Epo and RGB-286649 was found to promote a strong activation of IL5R reporter expression in approximately 25% of the cells. In this particular experiment, the efficiency of infection with the ABL-expressing virus was approximately 25%, suggesting nearly quantitative activation of the reporter in infected cells. Similar results were observed for other pairwise interactions (data not shown). These experiments established that viral transduction and integrated expression of a gp130-target fusion protein can lead to a robust activation of the integrated STAT3-responsive IL5R reporter gene in these cells.

Next, we explored the use of MASPIT in cDNA library screening and in the de novo identification of small molecule target proteins. A cDNA library was constructed from HEK293 mRNA in a retroviral vector (this library contained >1 × 10^8 primary clones, >99% of which contained inserts). The IL5R reporter cells were infected with the retroviral library and subjected to various cycles of enrichment for MFC-dependent IL5R-positive cells (see Experimental Procedures), followed by flow cytometric single-cell sorting into 96-well microtiter plates (Figure 4B). Individual cell populations were subsequently screened for MFC- and Epo-dependent

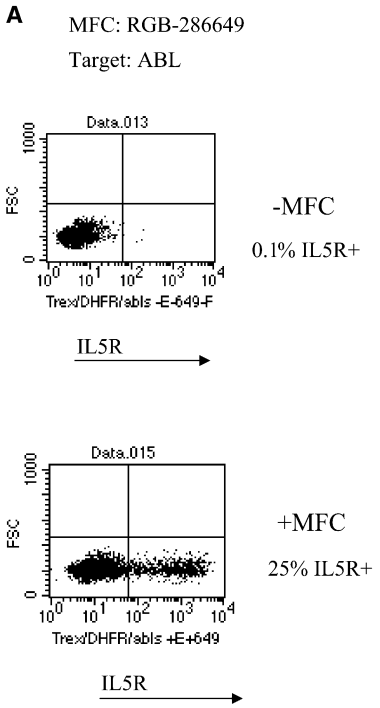

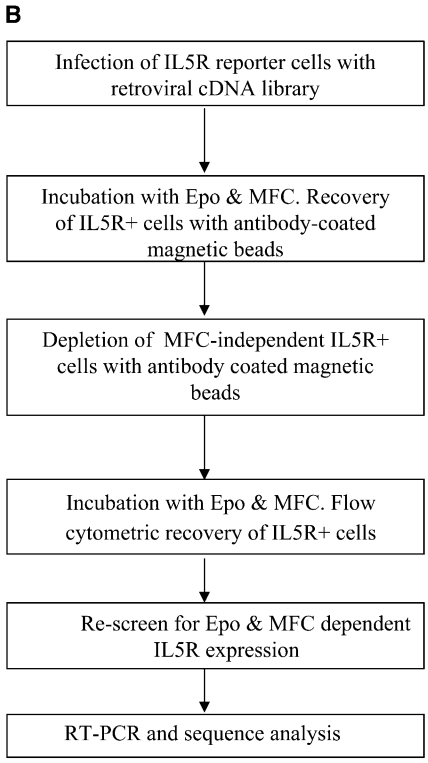

C

cDNA Library Screen Results for RGB-286649 (PD-173955 MFC)

Target gene identified with MASPIT	In vitro kinase inhibition by PD173955 (IC50 μM)
Lyn	<0.001
Fyn	0.001
FGFR1	0.016
EphA2	0.02
EphB1	0.117
EphB2	0.018
EphB4	0.034
GAK	nd
ABL	<0.003

Figure 4. MASPIT Proteome Screening

(A) Induction of MASPIT signaling with integrated system components. The cell line T-Rex44-eDHFR-gp130-ABL, which carries integrated copies of transgenes encoding the EpoR-LepRF3-DHFR fusion protein, gp130-ABL target protein, and an IL5R reporter, was exposed to the RGB-286649 (0.30 μM) MFC in the presence of Epo for 24 hr or left untreated. Cells were stained with an anti-IL5R antibody and positive cells were quantified by flow cytometry.

(B) MASPIT cDNA library screening workflow.

(C) Kinases identified in a proteome library screen with the MFC RGB-286649.

reporter activation by fluorescence activated cell sorting (FACS).

Figure 4C shows the results of a cDNA library screen we performed with RGB-286649, the MFC incorporating the ABL tyrosine kinase inhibitor PD173955 (see Figure 2 for compound details). In this screen, we identified a number of different tyrosine kinases as well as one Ser/Thr kinase. Only kinases were identified in this screen. PD173955 is a member of the pyrido[2,3-d]pyrimidine chemical class. Compounds of this class were initially developed as broadly active inhibitors of several tyrosine kinases, including SRC-like kinases and fibroblast growth factor receptors (FGFRs) [25, 26, 31, 32]. Here we identified the SRC kinases LYN and FYN, as well as FGFR1, as targets of PD173955 in MASPIT. We also identified several additional kinases that, to our knowledge, had not previously been reported as targets of this compound—such as various ephrin receptors (Eph receptor tyrosine kinases) and cyclin G-associated kinase (GAK). PD173955 was found to potently inhibit the in vitro kinase activity of these enzymes (Figure 4C; GAK was not evaluated). These findings validate the MASPIT results and further support the conjecture that this compound is less selective than previously known. Interaction of the MFC for PD173955 with specific ephrin receptors was also observed with Y3H in a directed array analysis using yeast cells expressing these target proteins (data not shown). These were, however, not identified in a Y3H cDNA library screen, although this employed a HeLa cell cDNA library rather than HEK293 cDNA library (data not shown). Future comparative studies might shed more light onto potential differences in target profiles that may be obtained with one or the other screening method, although such differences are likely to vary from case to case due to the multiple variables that generally govern cDNA library screening results. Some of the targets identified in the MASPIT screen (including GAK), albeit not all (e.g., EphA2, B1, and B2), were recently also identified and validated for a molecule highly related to PD173955, using a biochemical approach to small molecule target identification [33].

Competition Assays and Determination of Small Molecule Targeting Potencies

If stimulation of reporter gene activation and expression by a hybrid ligand is mediated by crosslinking of DHFR and target fusion proteins, then the individual components of that ligand (i.e., MTX and the small molecule of interest) should act as competitive inhibitors of reporter expression. Competition assays should provide (1) a means to directly validate a candidate small molecule-protein interaction (e.g., such as identified in a cDNA library screen) and (2) an opportunity to compare and rank small molecules on the basis of their relative ability to displace a hybrid ligand from its target protein(s) in intact cells. Such cellular targeting potency is

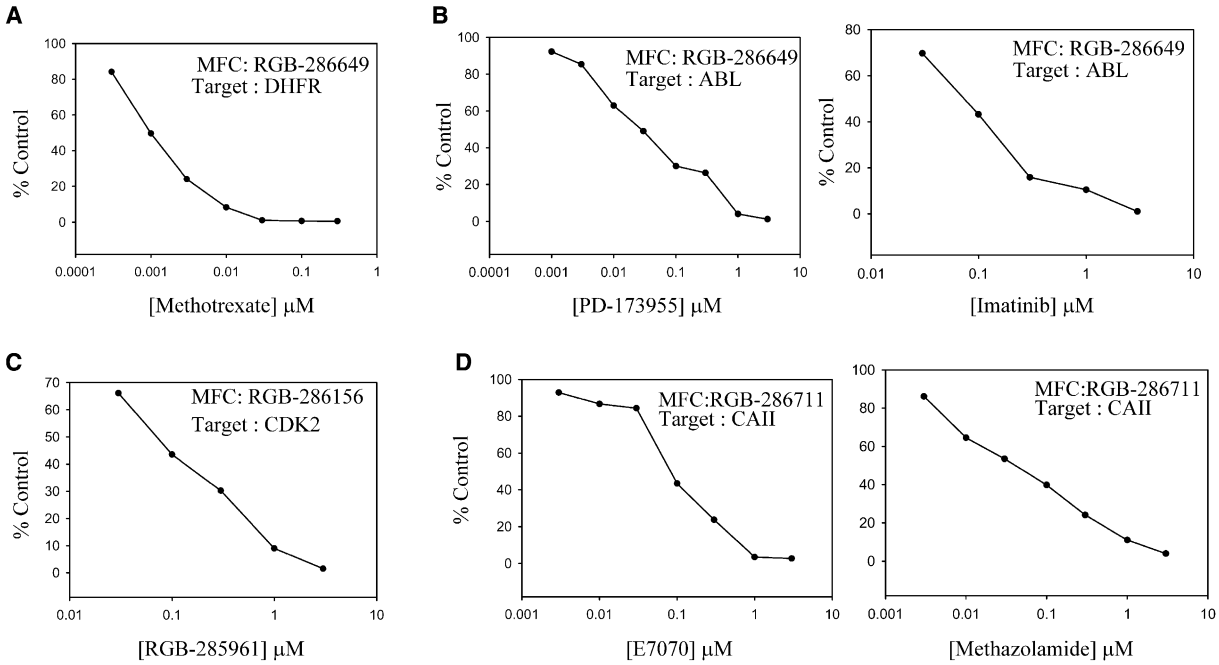

Figure 5. Competition Assays and Determination of Small Molecule Targeting Potencies

HEK293T cells were transiently cotransfected with the standard components (EpoR-LepRF3-DHFR bait, the rPAP-luciferase reporter, and the β-galactosidase control vector) and the indicated gp130-target vectors. Transfected cells were exposed for 24 hr to Epo and the indicated MFC in the presence or absence of a competing small molecule. The normalized luciferase activity as a function of the fully induced control (i.e., MFC and Epo) is presented.

(A) MTX competes with RGB-286649 (0.01 μM) for binding to DHFR.

(B) PD-173955 and imatinib compete with RGB-286649 (0.01 μM) for binding to ABL.

(C) The small molecule CDK inhibitor, RGB-285961, competes with RGB-286156 (0.2 μM) for binding to CDK2.

(D) Small molecule CAII inhibitors, E7070 and methazolamide, compete with RGB-286711 (0.1 μM) for binding to CAII.

expressed as an EC_{50} value, the compound concentration giving half-maximal inhibition of reporter expression that is observed in response to an MFC (competition is performed within the linear/dynamic range of the assay as relates to the MFC; see, for example, Figure 3). Below we summarize results of various competition experiments.

Figure 5A shows that MTX inhibits RGB-286649 (MFC of the ABL inhibitor PD173955)-induced reporter expression in a dose-dependent fashion, with an EC_{50} value of ~1 nM. This value is significantly below the concentration at which antiproliferative effects of MTX were apparent (see Figure 2; IC_{50} is > 3 μM at 24 hr incubation), suggesting that inhibition of reporter expression was due to binding of MTX to the DHFR fusion protein and not to an unspecific loss in cell viability. An EC_{50} value of ~1 nM also suggests that MTX retains a high relative affinity for the DHFR fusion protein in these cells.

Figures 5B–5D outline competition experiments with kinase and carbonic anhydrase small molecule inhibitors. A dose-dependent inhibition of MFC-induced luciferase reporter expression was observed for these competitor molecules, with EC_{50} values in the range of 28–80 nM. It should be noted that in a situation where the target protein is present in excess, an EC_{50} value might underestimate the cellular potency of a competitor. This is because it would underestimate the component of its value that reflects binding affinity (i.e., binding could be stronger than would appear from the assay). Thus, for the experiments shown in Figure 5, we tried to achieve assay conditions in which the target protein was not in excess (these conditions are generally easily achieved; see Figure 3C). Figure 6A shows control experiments that further demonstrate in two ways that inhibition of MASPIT signaling reflects inhibition of MFC-target protein interaction by the competitive compounds. First, antiproliferative effects were apparent only at much higher concentrations (IC_{50}s > 3 μM, 24 hr incubation), arguing against a nonspecific effect related to changes in cell viability. Second, compounds did not inhibit leukemia inhibitory factor (LIF)-induced JAK/STAT3 signaling. LIF induces JAK/STAT3 signaling via endogenous gp130 in HEK293 cells. Accordingly, at the tested concentration of 100 nM (which exceeds any of the EC_{50} values), the competitor compounds did not significantly inhibit LIF-induced STAT3 phosphorylation. In contrast, a known inhibitor of JAK/STAT signaling, cucurbitacin [34, 35], significantly inhibited LIF-induced STAT3 phosphorylation (99.3% inhibition at 5 μM). Importantly, competitor compounds (100 nM) also did not inhibit LIF-induced expression of a stably integrated STAT3-responsive IL5R reporter gene in HEK293 cells.

Individual EC_{50} values are summarized in Figure 6B. For comparison, compound IC_{50} values for in vitro inhibition of enzymatic activities of purified proteins are also shown. A wide spread in EC_{50}/IC_{50} ratios was observed for the different compounds. If one assumes that binding efficiency generally correlates well with potency of enzyme inhibition (for example, see study by Fabian et al. [4]), these results would suggest that

A

Compound	HEK293T IC50 (μM)	LIF Induction	%STAT3-Y705-P+	%IL5R + cells
None	-	-	0.1-0.8	0.4
None	-	+	97-100	17
Cucurbitacin		+	0.7	nd
Methotrexate	>3	+	100	18
RGB-285961	>3	+	100	17
Imatinib	>3	+	84	17
PD-173955	>3	+	90	19
E7070	>3	+	98	18
Methazolamide	>3	+	100	17

B

Compound	Target	EC50 (μM)	IC50 (μM)	EC50/IC50
Methotrexate	DHFR	0.001	nd	
RGB-285961	CDK2	0.07	0.02	3.5
Imatinib	ABL	0.07	0.372	0.2
PD-173955	ABL	0.028	< 0.003	>9.3
E7070	CAII	0.08	0.007	11.4
Methazolamide	CAII	0.04	0.014	2.9

C

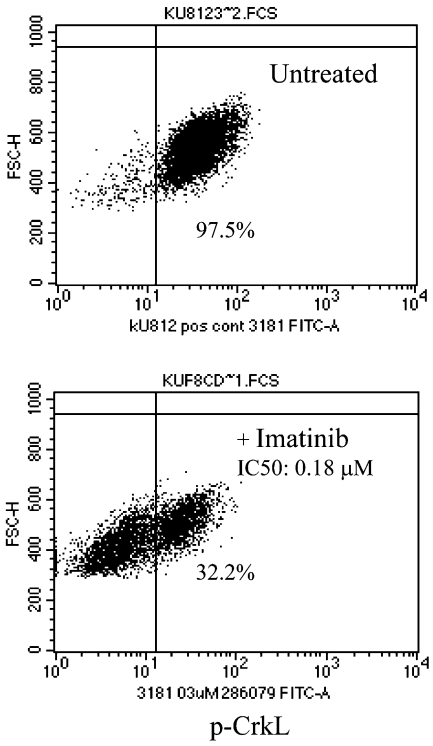

Figure 6. Small Molecule Inhibition of MASPIT Signaling Reflects Inhibition of MFC-Target Association

(A) Compounds used in competition experiments (Figure 5) are not cytotoxic to HEK293T cells (24 hr exposure, SRB assay), and do not inhibit LIF-induced phosphorylation of STAT3 (HEK293T cells) or STAT3-dependent induction of IL5R expression in HEK293 cells (T-Rex-44). The phosphorylation of STAT3 and expression of IL5R was measured following 15 min and 16 hr of exposure, respectively, to LIF in the presence or absence of a particular small molecule (cucurbitacin at 5 μM, all other compounds at 0.1 μM).

(B) Comparison of MASPIT EC_{50} values with IC_{50} values for in vitro enzyme inhibition. IC_{50} for methazolamide was taken from Abbate et al. [30]. The IC_{50} value for imatinib is in the range of previously reported values [40].

(C) Inhibition of cellular CrkL phosphorylation by imatinib. KU-812 leukemia cells, which express BCR-ABL, were either left untreated or exposed to a dose range of imatinib for 24 hr. The percentage of cells expressing phosphorylated CrkL was determined by flow cytometry. nd, not determined.

some compounds were qualitatively more effective than others in targeting their receptors in a cellular environment (e.g., see results for imatinib versus PD13955). Cellular targeting efficiency may depend on numerous factors, including cell permeability, conformation of the target protein, relative abundance of a target protein compared to other target proteins, and cellular constituents that may affect protein binding. Given that a MASPIT EC_{50} value is likely to integrate many such variables, it could provide a novel means to evaluate the intracellular targeting efficiency of a small molecule (and compare it to others). This supposition is further supported by the results obtained with the ABL inhibitors PD173955 and imatinib, which show that an EC_{50} value for a specific target protein (ABL in this case) can correlate well with the cellular activity of a compound that is mediated by such a target. Accordingly, imatinib was found to exhibit an EC_{50} value for ABL (70 nM) which correlated well with its IC_{50} for inhibition of BCR-ABL-driven phosphorylation of CrkL in KU812 leukemia cells (180 nM; Figure 6C) and IC_{50} for inhibition of BCR-ABL-dependent KU812 cell viability (137 nM). The EC_{50} for PD173955 (28 nM) was also similar to its IC_{50} for inhibition of KU812 cell viability (16 nM).

Rapid Kinetics Competition Assays

As described above, high levels of transcriptional induction and expression of a STAT3-responsive reporter might require exposure of cells to an MFC for up to 24 hr. A more rapid readout of an interaction might be preferable for competition assays, in particular for compounds that might exhibit cytotoxic activities or inhibit STAT3-induced reporter expression indirectly (i.e., by a mechanism other than direct inhibition of MFC-target interaction). In Figure 6, we describe the use of a STAT3 phosphorylation assay to monitor LIF-induced activation of JAK2/STAT3 signaling. Here we show that STAT3 phosphorylation also occurs rapidly in response to an MFC-induced small molecule-protein interaction in MASPIT, providing an assay format that might be

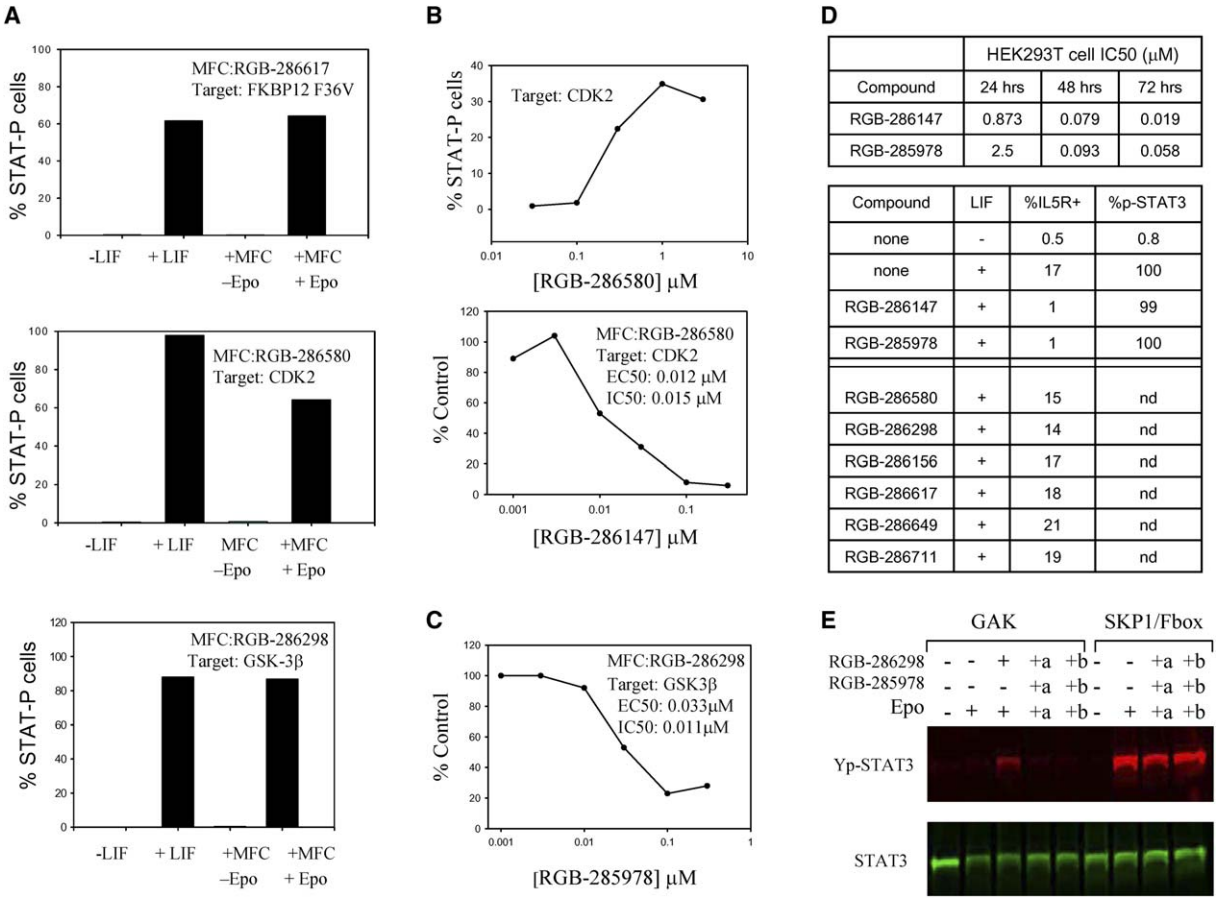

	HEK293T cell IC50 (μM)		
Compound	24 hrs	48 hrs	72 hrs
RGB-286147	0.873	0.079	0.019
RGB-285978	2.5	0.093	0.058

Compound	LIF	%IL5R+	%p-STAT3
none	-	0.5	0.8
none	+	17	100
RGB-286147	+	1	99
RGB-285978	+	1	100
RGB-286580	+	15	nd
RGB-286298	+	14	nd
RGB-286156	+	17	nd
RGB-286617	+	18	nd
RGB-286649	+	21	nd
RGB-286711	+	19	nd

Figure 7. Rapid Kinetics Competition Assay

(A) Rapid induction of STAT3 phosphorylation in MASPIT. HEK293T cells were transiently transfected with vector encoding EpoR-LepRF3-DHFR and a vector encoding gp130-FKBP12^{F36V} (top), gp130-CDK2 (middle), or gp130-GSK3β (bottom), and exposed to the indicated MFC (1 μM each) in the presence or absence of Epo for 15 min. The percentage of p-STAT3-positive cells was then determined by flow cytometry.

(B and C) MASPIT competition assays using the p-STAT3 readout. Cells were transiently transfected with EpoR-LepRF3-DHFR vector and the indicated gp130-target vector. (B) Top: dose-dependent induction of STAT3 phosphorylation with MFC RGB-286580 (15 min exposure in the presence of Epo). Bottom: competition assay (MFC, RGB-286580 at 1 μM) with the small molecule CDK inhibitor RGB-286147 (15 min exposure time).

(C) Competition assay (MFC, RGB-286298 at 1 μM) with the GSK3β inhibitor RGB-285978 (15 min exposure time).

(D) Compound inhibition of HEK293T cell proliferation, as determined with the SRB assay (similar results were obtained with a viability assay; data not shown). Induction of STAT3 phosphorylation or induction of the STAT3-responsive IL5R reporter was determined after 15 min or 16 hr exposure, respectively, to LIF in the presence or absence of the indicated compounds at a concentration of 100 nM for RGB-285978 or RGB-286147, or 1 μM for the indicated MFCs (all other compounds).

(E) RGB-285978 inhibits MASPIT signaling (target: GAK) but not MAPPIT signaling (SKP1/F box protein-protein interaction). Here we used HEK293 cells stably expressing the EpoR-LepRF3-DHFR bait and the gp130-GAK prey (left half of gel for MASPIT experiment) or HEK293 cells stably expressing EpoR-LepRF3-SKP1 and gp130-F box fusion proteins (right half of gel for MAPPIT experiment). F box is a protein of unknown function that we identified in a MAPPIT cDNA library screen with SKP1 (data not shown). Two experimental setups were used: (1) RGB-285978 competitor was added subsequent to incubation of cells with MFC (columns marked with +a; cells were incubated for 30 min with MFC, followed by addition of RGB-285978 for 30 min, followed by addition of Epo for 60 min); (2) all reagents were added simultaneously and cells were incubated for 60 min (columns marked +b). The same order of addition of compounds had no effect on Epo-stimulated STAT3 phosphorylation in the SKP1/F box MAPPIT setting. pSTAT3 and STAT3 levels were determined by immunoblotting with antibodies specific for these proteins.

preferred over the transcription-based readout assay for use with competitive compounds.

Accordingly, Figure 7A shows that a pronounced Epo-dependent induction of STAT3 phosphorylation is observed in transiently transfected HEK293T cells in response to a 15 min exposure to an MFC, as shown for RGB-286617 (target: FKBP12^{F36V}), RGB-286580 (target: CDK2), and RGB-286298 (target: GSK3β). Induction of STAT3 phosphorylation was generally comparable in magnitude to that observed for untransfected cells in response to LIF. As shown for RGB-286580, induction of STAT3 phosphorylation was dose-dependent (Figure 7B). Figures 7B and 7C show results of competition experiments with the kinase inhibitors RGB-286147 (target: CDK2) and RGB-285978 (target: GSK3β). For RGB-286147, an EC_{50} (12 nM) comparable to the IC_{50} (15 nM) for in vitro CDK2 inhibition was determined (Figure 7B). For the GSK3β inhibitor RGB-285978, an EC_{50} (33 nM) comparable to the IC_{50} (11 nM) for inhibition of GSK3β kinase activity in vitro was obtained (Figure 7C). Neither

of these kinase inhibitors repressed LIF-induced STAT3 phosphorylation (Figure 7D), suggesting that these compounds directly inhibited the respective MFC-target interactions. Furthermore, as previously shown to be the case for imatinib and its target ABL (Figure 6), these results also suggest that these compounds target their receptors in cells with high efficiency (at least when these are expressed as gp130 fusion proteins).

In contrast to their lack of inhibition of LIF-induced STAT3 phosphorylation upon short-term exposure (100 nM, 15 min), RGB-286147 and RGB-285978 abrogated LIF-induced expression of the STAT3-responsive IL5R reporter gene in HEK293 cells upon longer term exposure (100 nM, 16 hr), as shown in Figure 7D. The cause of these inhibitory effects could be their cytotoxic activities and/or inhibition of STAT3-mediated transcription. Both RGB-286147 and RGB-285978 are potent cytotoxic agents against many different cell types ([15]; data not shown), including HEK293T cells (Figure 7D). Although the potent antiproliferative/cytotoxic effects of these compounds were apparent only by 48 hr (Figure 7D), microscopic analysis revealed that by 24 hr, cells began to round up and to display significant changes in morphology (data not shown), suggesting that adverse effects on the viability of these cells might have initiated at earlier time points. Alternatively, inhibition of LIF-induced IL5R expression could have involved transcriptional effects, as both of these compounds are potent inhibitors of cyclin-dependent kinases that are known to be involved in gene transcription/elongation (e.g., CDK7 and CDK9; [13, 15], and data not shown). Thus, RGB-286147 and RGB-285978 are good examples of compounds for which a MASPIT STAT3 phosphorylation assay but not a MASPIT STAT3-dependent reporter transcription assay would be suitable for competition experiments and determination of EC_{50} values.

As shown in Figure 7D, none of the MFCs used in this study inhibited LIF-induced IL5R expression, nor did they exhibit adverse effects on cell proliferation and viability (Figure 2)—which is consistent with the observations that these MFCs produced robust MASPIT signals. Interestingly, these observations were also made for the MFCs of RGB-286147 and RGB-285978, compounds which did inhibit LIF-induced IL5R expression and displayed cytotoxic activities. It is conceivable that modification of these compounds (linker addition and coupling to MTX) resulted in the loss of specific interactions mediating cytotoxic activities of these compounds. Alternatively, it is also conceivable that such modifications, in particular coupling with MTX (which results in a significantly bulkier molecule), simply reduces the affinity of a small molecule for a target protein but not its overall interaction fingerprint—and that interactions of reduced affinity are still detectable with MASPIT. For instance, with respect to RGB-286147 and the respective MFC RGB-286156, we favor the latter scenario. In this case, as shown previously [15], addition of the PEG linker does not significantly influence the biological potency of this pyrazolopyrimidone. However, subsequent coupling to MTX does reduce its in vitro kinase inhibitory potency (e.g., IC_{50} for CDK2/cyclinE was found to be $\sim$200 nM for RGB-286156, compared to an IC_{50} of $\sim$15 nM for RGB-286147). Despite this effect, interaction with CDK2 can easily be detected with Y3H and MASPIT. Furthermore, as previously shown [15], RGB-286156 interacts in Y3H with all the CDK/CRK kinases that RGB-286147 and related analogs interact with in vitro (with the exception of CDK7, which is likely to require a trimeric enzyme complex not replicated in yeast cells). Thus, although chemical modification might affect the biological potency of a compound, it may not necessarily change its target profile.

Screening for Interaction Modifiers Using Stably Integrated MASPIT System Components

The experiments described above employed HEK293T cells that were transiently transfected with expression vectors encoding specific fusion proteins. Here we show that HEK293 cells stably expressing EpoR-LepRF3-DHFR and gp130 fusion proteins (such as those identified in a cDNA library screen) can also be used to perform competition experiments with a STAT3 phosphorylation assay. In this study, we did not use flow cytometric detection of pY-STAT3-positive cells, but an immunoblot assay for quantitation of relative cellular levels of pY-STAT3 as compared to total cellular STAT3 levels. As outlined in Figure 7E, RGB-286298 induced STAT3 phosphorylation in an Epo-dependent fashion as a result of its interaction with a gp130-GAK target protein (we identified GAK as a novel kinase target of this compound in a MASPIT cDNA library screen similar to that described in Figure 4B). No induction of STAT3 phosphorylation was observed in the presence of the competitor compound RGB-285978. Interestingly, RGB-285978 repressed STAT3 phosphorylation irrespective of whether it was added simultaneously with the MFC and Epo (lanes marked with +b) or subsequent to preincubation of cells with the MFC alone (30 min; lanes marked with +a), that is, conditions in which an MFC-target complex would be allowed to form prior to addition of competitor compound and subsequent stimulation with Epo. These different experimental setups could be used to determine whether a competitor compound would be able to interfere with the formation of and/or disrupt a small molecule-protein interaction. The inhibition of STAT3 phosphorylation by RGB-285978 under both experimental setups was specific, as indicated by the lack of effect of RGB-285978 (even at high concentration, 400 nM) on the Epo-induced STAT3 phosphorylation in the context of a MAPPIT protein-protein interaction (SKP1/F box: the F box protein was identified as a novel target protein in a MAPPIT cDNA library screen with SKP1 as a bait; data not shown). We have previously shown that RGB-285978 also does not inhibit LIF-induced STAT3 phosphorylation (Figure 7D). Collectively, these results show that a STAT3 phosphorylation assay may be used with both MASPIT and MAPPIT to rapidly screen for modifiers of small molecule-protein or protein-protein interactions, respectively.

Discussion

Chemical dimerizers have been widely used to temporally control the dimerization of specific proteins and the activity of signaling pathways in intact cells [36, 37]. Y3H extended the scope of chemical dimerizers to proteome-wide identification of small molecule targets [3, 12, 13, 15]. The MASPIT system described here

further expands the range of applications of chemical dimerizers. It provides a complementary method to Y3H for proteome cDNA library screening and target identification. In addition, MASPIT provides an assay platform for determining specificity and potency with which unmodified small molecules interact with target proteins in intact cells, and a new approach to compare and contrast biological activity profiles of compounds of various chemotypes and modes of action.

The multiple counterscreening options and quality control measures that can be exercised in the monitoring of MASPIT signaling events ought to contribute to a high level of confidence with which small molecule-protein interactions can be identified and characterized. An example of this is the cDNA library screen for the ABL kinase inhibitor PD173955, in which only kinases were identified, all of which could be independently confirmed (we have made similar observations for other compounds, including compounds that are not kinase inhibitors; M.C. and N.K., unpublished observations). The PD173955 interaction results also suggest that the pyrido[2,3-d]pyrimidine kinase inhibitor scaffold constitutes a core structure with potential for the rational design of ephrin receptor tyrosine kinase inhibitors. Various members of this kinase subfamily have been implicated in the regulation of numerous biological processes, including disease pathogenesis (e.g., cancer).

By enabling the characterization of targeting potencies, and thereby also a ranking of compounds based on both qualitative as well as quantitative differences in their target interaction fingerprints, MASPIT further expands the scope of compounds that can be studied with a 3H system. An important difference between determination of EC_{50} values using MASPIT and in vitro K_D or IC_{50} determinations is that EC_{50} values also reflect variables associated with compound bioavailability and intracellular targeting efficacy, such as: (1) compound uptake, compartmentalization, and stability; (2) the effect that binding of compound to other cellular targets might have on its interaction with the "intended" target; (3) effects of certain intracellular molecules on target binding (e.g., ATP, which is present at high concentrations in cells, competes with kinase inhibitors for binding to the active site of the enzyme [38]); and (4) effects that posttranslational modifications of the target, or its association with other proteins, might have on compound binding. Similar factors can result in shifts in IC_{50} values (in vitro versus cellular), as observed when comparing in vitro enzyme inhibition values with data on inhibition of enzyme-catalyzed substrate modification in intact cells (see PD173955 and imatinib examples in this study). One caveat with the interpretation of MASPIT EC_{50} values is that they reflect the targeting efficacy of a compound for a fusion protein (gp130 fusion). This is also the case with other assays, such as in vitro enzyme assays or phage display, which largely make use of recombinant fusion proteins. However, it appears that in many instances the intrinsic affinity of a small molecule for a recombinant versus nonrecombinant target protein is similar. Notwithstanding this potential caveat, the results of our study suggest that MASPIT EC_{50} values can be good indicators of the relative efficacies with which one or more compounds target a specific protein or subset of proteins in intact cells, thereby providing a more direct link to phenotypic data. The STAT3 phosphorylation assay would also enable the analysis of compounds with cytotoxic activities, which could be important for the analysis of certain anticancer agents. Thus, by enabling a quantitative rather than strictly qualitative mapping of small molecule-protein interaction fingerprints, MASPIT could facilitate the tracing of a therapeutic or biological effect of a compound to one or more of its molecular targets, thereby also facilitating strategies for the optimization of a compound for activity against a rationally selected subset of targets. Quantitative target fingerprinting might also prove useful in the recognition of potential new therapeutic applications of a small molecule or chemical class.

As shown in this study, MASPIT signaling events can readily be assessed by monitoring changes in the state of STAT3 phosphorylation, irrespective of whether MASPIT system components are expressed transiently or constitutively (from stably integrated transgenes). Transient expression studies are useful for performing competition experiments without the need for selecting stable integrants. In contrast, cells with integrated transgenes ought to be more appropriate if a larger number of compounds are to be screened for interaction modifier activity. The screening approaches described here would support limited throughput screening of compounds that interfere with or disrupt specific MFC small molecule-protein interactions. This would be a typical scenario for many lead optimization efforts. A high-throughput STAT3 phosphorylation assay, for instance a pY-STAT3 cytoblot assay [35], would further increase the utility of MASPIT in larger scale compound-screening campaigns. A high-throughput pY-STAT3 assay should similarly expand the range of applications of MAPPIT or reverse-MAPPIT in screening for protein-protein interaction modifiers. In summary, our study suggests that MASPIT has potential for broad applications in chemical biological research and drug discovery.

Significance

In this study we have described the development and applications of MASPIT, a three-hybrid system for small molecule-protein interaction profiling in mammalian cells. Our results show that MASPIT can be used with a variety of small molecule chemotypes and target classes, that it can be used in random proteome screens for the de novo identification of small molecule protein targets, and that it can be used to determine the targeting potencies of small molecules for specific targets in intact cells. The MASPIT system should prove useful in (1) characterizing the target spectra and selectivity profiles of small molecules, (2) mechanism of action studies attempting to link cellular targets to therapeutic/phenotypic effects of small molecules, and (3) uncovering potential novel therapeutic applications of drugs or drug candidates.

Experimental Procedures

MFC Synthesis

The chemical synthesis of the MFCs RGB-286156 and RGB-286580 has been described previously [13, 15]. The same strategy was used for synthesis of other MFCs.

Cell Culture and Proliferation Assays

HEK293T cells and the HEK293 reporter cell line, T-Rex44-eDHFR [22], were maintained in Dulbecco's modified Eagle's medium (DMEM) supplemented with 10% fetal calf serum (FCS). Cellular proliferation was determined with the sulforhodamine B, SRB, assay [39]. Cellular viability was determined with the CellTiterGlo luminescent cell viability assay according to the manufacturer's specifications (Promega).

Bait and Prey Constructs

The pSEL1 and pMG1 vectors for the transient expression of EpoR-LepRF3 and gp130 fusion proteins, respectively, have been previously described [18]. The pCel1f vector, based on the cDNA5/FRT vector, and used for directed integrated expression, has also been described [20]. The bait plasmid pSEL-eDHFR was generated by cloning the *E. coli* DHFR gene into pSEL using pBYK-DHFR [13] as a template. pCel1f-eDHFR was constructed by ligating eDHFR to the SacI and NotI sites of pCel1f. The CDK2, GSK3β, $FKBP12^{F36V}$, and carbonic anhydrase II (CAII) target plasmids were generated by subcloning the coding regions of these genes into pMG1. The ABL target construct was generated by cloning the kinase domain of ABLI (amino acids 246–532). See Appendix 2 (in the Supplemental Data available with this article online) for details of cloning. All primers used in this study are listed in Appendix 1.

Construction of Cell Lines

The T-Rex44-eDHFR cell line was created from T-Rex44 by recombining pCel1f-eDHFR into the FRT site. T-Rex44 has been previously described [18, 22]. Integration of the expression cassette using the flp-in system was done according to the manufacturer (Invitrogen). T-Rex44-eDHFR-ABL was created from T-Rex44-eDHFR. Ecotropic virus was prepared from pBG1-ABL and used to infect T-Rex44-eDHFR at a one-half dilution. The rate of infection was presumed to be 25% based on parallel infections with control vectors.

Transfections and MASPIT Reporter Assays/Competitions

HEK293T cells were grown to about 60% confluency in DMEM 10% FCS and transfected with 100 ng of each plasmid of the standard components (constructs carrying the EpoR-LepRF3-DHFR bait, the rPAP1-luciferase reporter, and the β-galactosidase control vectors) as well as the indicated gp130-target vector with TransIT-293 (Mirus, MIR2700). For induction of the MASPIT system, transfected cells were cultured in fresh media containing recombinant human erythropoetin (Epo) (5 units/ml of culture media; R&D Systems, 287-TC) in the presence of MFC for an additional 24 hr. In the standard competition assay, the MASPIT system was induced by the simultaneous exposure of transfected cells to Epo, the MFC, and the competitor compound for 24 hr. Cell lysates were prepared and β-galactosidase normalized luciferase activity was determined (Promega, E1501 and E2000). Variation in the MASPIT signal between wells transfected with the identical plasmid/lipid mixture was routinely found to be less than 10%. For reporter induction with leukemia inhibitory factor (LIF; Chemicon International, Lif1010), cells were treated with 1 ng/ml cytokine for 15 min (STAT3-Y705 detection) or 16 hr (IL5R detection).

Enzymatic Assays

CAII assays were performed at CEREP (Paris). CDK2 kinase assays were done as previously described [28]. All other kinase assays were performed at Upstate (Dundee, UK).

Western Blot Analysis

Western blot analysis was performed using standard procedures; see Appendix 2 for experimental details. The gp130-CDK2 fusion protein was detected with an anti-gp130 rabbit polyclonal antibody (Upstate). STAT3 was detected with a mouse anti-phospho-STAT3(Y705) antibody (Upstate) and a rabbit anti-STAT3 antibody (Santa Cruz Biotechnology).

Flow Cytometric Detection of p-STAT3 and p-CrkL

HEK293T cells were fixed and permeabilized for staining with the PE-conjugated anti-phospho-STAT3 (Y705) antibody (BD Biosciences, 612569). KU-812 cells were fixed and permeabilized for staining with an anti-p-CrkL antibody (Cell Signaling, 3181) and FITC-labeled secondary antibody (BD Biosciences, 554020). The stained cells were analyzed on a BD FACS Canto flow cytometer. See Appendix 2 for details.

cDNA Library Construction

Construction of the HEK293T cDNA library was done using standard procedures with random and oligo dT-primed cDNAs synthesized using the Superscript Choice system (Invitrogen). The library vector, pLN-CD90-CMV-gp130-ccdB, was constructed from pLNCX2 (Clontech). See Appendix 2 for details.

cDNA Library Screen and IL5R Staining

T-Rex44-eDHFR cells (4.4×10^8 cells) were infected with a retroviral cDNA library at a rate of 25% (infection efficiency). After 24 hr, the media was replaced with fresh media and the cells were allowed to recover for an additional 24 hr. Cells were stimulated with RGB-286649 (150 nM) and Epo (3 U/ml) for 24 hr and then stained for expression of the IL5R. The α-IL5R antibody (hybridoma 16-4 [22]) was used at 1.0 μg/ml. The secondary antibody was a PE-conjugated goat α-mouse IgG1 (Molecular Probes; used at 1.5 μg/ml). IL5R-positive cells were then either quantified by FACS or enriched on α-PE magnetic beads (500 μl) (StemCell Technologies). In the cDNA library screen, the IL5R-positive cells were enriched on five LS columns (Miltenyi). The cells were eluted through removal of the magnetic field and were allowed to recover. To deplete background due to constitutive activation of the IL5R reporter, cells were stained for expression of IL5R in the presence of Epo but absence of RGB-286649 and then reapplied to an LS column. The flow through was collected and the cells were allowed to recover. The recovered cells were stimulated with Epo and RGB-286649 and individual IL5R-positive cells were seeded into 96-well plates using a flow cytometer. Alternatively, IL5R-positive cells were enriched an additional time using α-PE magnetic beads, allowed to recover, and then seeded into 96-well plates using a flow cytometer. The cell lines that grew from the 96-well plate were retested for Epo- and RGB-286649-dependent IL5R expression by flow cytometry. Alternatively, immunological detection of the IL5R can be performed with a dot blot assay. The cDNA harbored in these cells was isolated by RT-PCR. RNA was isolated using an RNAeasy kit (Qiagen) and RT-PCR was performed using a One Step RT-PCR kit (Qiagen) with primers gp130F and 3′LNCX2-R1.

Supplemental Data

Supplemental Data contain experimental procedures, including oligonucleotide sequences and antibodies, and are provided in Appendices 1 and 2, which can be found with this article online at http://www.chembiol.com/cgi/content/full/13/7/711/DC1/.

Acknowledgments

We thank Drs. Margaret Lee Kley and David Bancroft for critical reading of the manuscript and many helpful comments.

Received: March 7, 2006
Revised: May 8, 2006
Accepted: May 10, 2006
Published: July 28, 2006

References

1. Burdine, L., and Kodadek, T. (2004). Target identification in chemical genetics: the (often) missing link. Chem. Biol. *11*, 593–597.
2. Daub, H., Godl, K., Brehmer, D., Klebl, B., and Muller, G. (2004). Evaluation of kinase inhibitor selectivity by chemical proteomics. Assay Drug Dev. Technol. *2*, 215–224.
3. Kley, N. (2004). Chemical dimerizers and three-hybrid systems: scanning the proteome for targets of organic small molecules. Chem. Biol. *11*, 599–608.
4. Fabian, M.A., Biggs, W.H., Treiber, D.K., Atteridge, C.E., Azimioara, M.D., Benedetti, M.G., Carter, T.A., Ciceri, P., Edeen, P.T., Floyd, M., et al. (2005). A small molecule-kinase interaction map for clinical kinase inhibitors. Nat. Biotechnol. *23*, 329–336.

5. Carter, T.A., Wodicka, L.M., Shah, N.P., Velasco, A.M., Fabian, M.A., Treiber, D.K., Milanov, Z.V., Atteridge, C.E., Biggs, W.H., III, Edeen, P.T., et al. (2005). Inhibition of drug-resistant mutants of ABL, KIT, and EGF receptor kinases. Proc. Natl. Acad. Sci. USA *102*, 11011–11016.
6. Toogood, P.L. (2005). The kinome is not enough. Chem. Biol. *12*, 1057–1058.
7. Zheng, X.S., Chan, T.F., and Zhou, H.H. (2004). Genetic and genomic approaches to identify and study the targets of bioactive small molecules. Chem. Biol. *11*, 609–618.
8. Kley, N., Ivanov, I., and Meier-Ewert, S. (2004). Genomics and proteomics tools for compound mode-of-action studies in drug discovery. Pharmacogenomics *5*, 395–404.
9. Jessani, N., and Cravatt, B.F. (2004). The development and application of methods for activity-based protein profiling. Curr. Opin. Chem. Biol. *8*, 54–59.
10. Predki, P.F. (2004). Functional protein microarrays: ripe for discovery. Curr. Opin. Chem. Biol. *8*, 8–13.
11. Fields, S., and Song, O. (1989). A novel genetic system to detect protein-protein interactions. Nature *340*, 245–246.
12. Licitra, E.J., and Liu, J.O. (1996). A three-hybrid system for detecting small ligand-protein receptor interactions. Proc. Natl. Acad. Sci. USA *93*, 12817–12821.
13. Becker, F., Murthi, K., Smith, C., Come, J., Costa-Roldan, N., Kaufmann, C., Hanke, U., Degenhart, C., Baumann, S., Wallner, W., et al. (2004). A three-hybrid approach to scanning the proteome for targets of small molecule kinase inhibitors. Chem. Biol. *11*, 211–223.
14. Lin, H., Abida, W.M., Sauer, R.T., and Cornish, V.W. (2000). Dexamethasone-methotrexate: an efficient chemical inducer of protein dimerization in vivo. J. Am. Chem. Soc. *122*, 4247–4248.
15. Caligiuri, M., Becker, F., Murthi, K., Kaplan, F., Dedier, S., Kaufmann, C., Machl, A., Zybarth, G., Richard, J., Bockovich, N., et al. (2005). A proteome-wide CDK/CRK-specific kinase inhibitor promotes tumor cell death in the absence of cell cycle progression. Chem. Biol. *12*, 1103–1115.
16. Daub, H., Specht, K., and Ullrich, A. (2004). Strategies to overcome resistance to targeted protein kinase inhibitors. Nat. Rev. Drug Discov. *3*, 1001–1010.
17. Blencke, S., Ullrich, A., and Daub, H. (2003). Mutation of threonine 766 in the epidermal growth factor receptor reveals a hotspot for resistance formation against selective tyrosine kinase inhibitors. J. Biol. Chem. *278*, 15435–15440.
18. Eyckerman, S., Verhee, A., der Heyden, J.V., Lemmens, I., Ostade, X.V., Vandekerckhove, J., and Tavernier, J. (2001). Design and application of a cytokine-receptor-based interaction trap. Nat. Cell Biol. *3*, 1114–1119.
19. Tavernier, J., Eyckerman, S., Lemmens, I., Van der Heyden, J., Vandekerckhove, J., and Van Ostade, X. (2002). MAPPIT: a cytokine receptor-based two-hybrid method in mammalian cells. Clin. Exp. Allergy *32*, 1397–1404.
20. Eyckerman, S., Lemmens, I., Lievens, S., Van der Heyden, J., Verhee, A., Vandekerckhove, J., and Tavernier, J. (2002). Design and use of a mammalian protein-protein interaction trap (MAPPIT). Sci. STKE *2002*, PL18.
21. Lemmens, I., Eyckerman, S., Zabeau, L., Catteeuw, D., Vertenten, E., Verschueren, K., Huylebroeck, D., Vandekerckhove, J., and Tavernier, J. (2003). Heteromeric MAPPIT: a novel strategy to study modification-dependent protein-protein interactions in mammalian cells. Nucleic Acids Res. *31*, e75.
22. Lievens, S., Van der Heyden, J., Vertenten, E., Plum, J., Vandekerckhove, J., and Tavernier, J. (2004). Design of a fluorescence-activated cell sorting-based mammalian protein-protein interaction trap. Methods Mol. Biol. *263*, 293–310.
23. Eyckerman, S., Lemmens, I., Catteeuw, D., Verhee, A., Vandekerckhove, J., Lievens, S., and Tavernier, J. (2005). Reverse MAPPIT: screening for protein-protein interaction modifiers in mammalian cells. Nat. Methods *2*, 427–433.
24. Clackson, T., Yang, W., Rozamus, L.W., Hatada, M., Amara, J.F., Rollins, C.T., Stevenson, L.F., Magari, S.R., Wood, S.A., Courage, N.L., et al. (1998). Redesigning an FKBP-ligand interface to generate chemical dimerizers with novel specificity. Proc. Natl. Acad. Sci. USA *95*, 10437–10442.
25. Wisniewski, D., Lambek, C.L., Liu, C., Strife, A., Veach, D.R., Nagar, B., Young, M.A., Schindler, T., Bornmann, W.G., Bertino, J.R., et al. (2002). Characterization of potent inhibitors of the Bcr-Abl and the c-kit receptor tyrosine kinases. Cancer Res. *62*, 4244–4255.
26. Nagar, B., Bornmann, W.G., Pellicena, P., Schindler, T., Veach, D.R., Miller, W.T., Clarkson, B., and Kuriyan, J. (2002). Crystal structures of the kinase domain of c-Abl in complex with the small molecule inhibitors PD173955 and imatinib (STI-571). Cancer Res. *62*, 4236–4243.
27. Markwalder, J.A., Arnone, M.R., Benfield, P.A., Boisclair, M., Burton, C.R., Chang, C.H., Cox, S.S., Czerniak, P.M., Dean, C.L., Doleniak, D., et al. (2004). Synthesis and biological evaluation of 1-aryl-4,5-dihydro-1H-pyrazolo[3,4-d]pyrimidin-4-one inhibitors of cyclin-dependent kinases. J. Med. Chem. *47*, 5894–5911.
28. Nugiel, D.A., Vidwans, A., Etzkorn, A.M., Rossi, K.A., Benfield, P.A., Burton, C.R., Cox, S., Doleniak, D., and Seitz, S.P. (2002). Synthesis and evaluation of indenopyrazoles as cyclin-dependent kinase inhibitors. 2. Probing the indeno ring substituent pattern. J. Med. Chem. *45*, 5224–5232.
29. Nugiel, D.A., Etzkorn, A.M., Vidwans, A., Benfield, P.A., Boisclair, M., Burton, C.R., Cox, S., Czerniak, P.M., Doleniak, D., and Seitz, S.P. (2001). Indenopyrazoles as novel cyclin dependent kinase (CDK) inhibitors. J. Med. Chem. *44*, 1334–1336.
30. Abbate, F., Casini, A., Owa, T., Scozzafava, A., and Supuran, C.T. (2004). Carbonic anhydrase inhibitors: E7070, a sulfonamide anticancer agent, potently inhibits cytosolic isozymes I and II, and transmembrane, tumor-associated isozyme IX. Bioorg. Med. Chem. Lett. *14*, 217–223.
31. Dorsey, J.F., Jove, R., Kraker, A.J., and Wu, J. (2000). The pyrido[2,3-d]pyrimidine derivative PD180970 inhibits p210Bcr-Abl tyrosine kinase and induces apoptosis of K562 leukemic cells. Cancer Res. *60*, 3127–3131.
32. Klutchko, S.R., Hamby, J.M., Boschelli, D.H., Wu, Z., Kraker, A.J., Amar, A.M., Hartl, B.G., Shen, C., Klohs, W.D., Steinkampf, R.W., et al. (1998). 2-substituted aminopyrido[2,3-d]pyrimidin-7(8H)-ones. Structure-activity relationships against selected tyrosine kinases and in vitro and in vivo anticancer activity. J. Med. Chem. *41*, 3276–3292.
33. Wissing, J., Godl, K., Brehmer, D., Blencke, S., Weber, M., Habenberger, P., Stein-Gerlach, M., Missio, A., Cotten, M., Muller, S., et al. (2004). Chemical proteomic analysis reveals alternative modes of action for pyrido[2,3-d]pyrimidine kinase inhibitors. Mol. Cell. Proteomics *3*, 1181–1193.
34. Sun, J., Blaskovich, M.A., Jove, R., Livingston, S.K., Coppola, D., and Sebti, S.M. (2005). Cucurbitacin Q: a selective STAT3 activation inhibitor with potent antitumor activity. Oncogene *24*, 3236–3245.
35. Blaskovich, M.A., Sun, J., Cantor, A., Turkson, J., Jove, R., and Sebti, S.M. (2003). Discovery of JSI-124 (cucurbitacin I), a selective Janus kinase/signal transducer and activator of transcription 3 signaling pathway inhibitor with potent antitumor activity against human and murine cancer cells in mice. Cancer Res. *63*, 1270–1279.
36. Schreiber, S.L. (1998). Chemical genetics resulting from a passion for synthetic organic chemistry. Bioorg. Med. Chem. *6*, 1127–1152.
37. Pollock, R., and Clackson, T. (2002). Dimerizer-regulated gene expression. Curr. Opin. Biotechnol. *13*, 459–467.
38. Knight, Z.A., and Shokat, K.M. (2005). Features of selective kinase inhibitors. Chem. Biol. *12*, 621–637.
39. Skehan, P., Storeng, R., Scudiero, D., Monks, A., McMahon, J., Vistica, D., Warren, J.T., Bokesch, H., Kenney, S., and Boyd, M.R. (1990). New colorimetric cytotoxicity assay for anticancer-drug screening. J. Natl. Cancer Inst. *82*, 1107–1112.
40. O'Hare, T., and Druker, B.J. (2005). BIRB-796 is not an effective ABL(T315I) inhibitor. Nat. Biotechnol. *23*, 1209–1210, author reply 1210–1211.